# Optimization Research of High-Speed Railway EMU Utilization Schedule Based on Three-Dimensional Space-Time Network

Mingjun Qian, Xin Huang, Mingli Li

*Abstract*—**With the continuous improvement of China High-Speed Railway network and the large number of EMUs being put into operation, it is essential to conduct in-depth research on the preparation and optimization of EMU operation schedules from the perspectives of energy consumption and carbon emissions during the operation and maintenance phases, in order to achieve the carbon peaking and carbon neutrality goals in the transportation sector. Firstly, addressing the space-time dynamic characteristics of EMU operation schedules, a three-dimensional space-time network model of EMU operation schedules is established by adding the maintenance status dimension to the traditional two-dimensional space-time network model. By utilizing the connection changes of different operational status arcs in the three-dimensional space-time network, important information such as the maintenance status, maintenance frequency, and carbon emissions can be clearly and effectively presented, thus fully and accurately describing the entire operation and maintenance process of the EMUs. Next, considering the maintenance requirements of the EMUs, connection time constraints, status arc occupation constraints, operation arc conflict resolution constraints, and other conditions, an optimization model for High-Speed Railway EMU operation schedules based on the three-dimensional space-time network is established. The objective is to minimize the total EMU operation time, reduce maintenance frequency, and achieve the balanced carbon emission level. A three-dimensional array coding NSGA-II genetic algorithm has been designed to solve the model. This algorithm employs a crossover strategy that retains cross information, maximizes the retention of non-cross information, and conditionally regenerates. Finally, the model and algorithm's effectiveness is verified using relevant data from the Beijing-Shanghai High-Speed Railway EMU operation schedules. The results indicate that the optimization model and algorithm, grounded in the three-dimensional space-time network, not only accurately depict the entire operation and maintenance lifecycle of the EMUs, but also significantly enhance their operational efficiency and benefits, reduce the number of EMUs in operation, and mitigate carbon emissions. This research can provide a valuable reference for High-Speed Railway operation and management departments in formulating or optimizing EMU operation schedules.**

***Keywords*: High-Speed Railway; EMU operation schedules; Space-Time Network; Carbon emissions; NSGA-II algorithm**

Manuscript received September 29, 2024; revised February 13, 2025.

This work was supported in part by Double First Class Major Scientific Research Project of Gansu Provincial Department of Education (GSSYLXM-04); Gansu Provincial Department of Education Higher Education Innovation Fund Project (2020A-038); Youth Fund Project of Lanzhou Jiaotong University (2014029).

Mingjun Qian is an Associate professor at School of Traffic and Transportation, Lanzhou Jiaotong University, Lanzhou 730070, China. (Corresponding author, e-mail: qianmingjun@mail.lzjtu.cn).

Xin Huang is a Postgraduate student at School of Traffic and Transportation, Lanzhou Jiaotong University, Lanzhou 730070, China. (e-mail: 1632296429@qq. com).

Mingli Li is a Postgraduate student at School of Traffic and Transportation, Lanzhou Jiaotong University, Lanzhou 730070, China. (e-mail: 1429471381@qq. com)

## I. Introduction

As China's High-Speed Railway network has surpassed 47,000 kilometers in total length, a large number of High-Speed EMUs are scheduled to operate and undergo maintenance every day. Throughout the entire lifecycle of high-speed railways, the operation and maintenance phase have the longest duration and the highest energy consumption, inevitably leading to significant indirect carbon emissions. Among these, the electricity consumed by the EMUs for traction and maintenance is the most energy-intensive.

Therefore, in response to the national "carbon emissions reduction and neutrality" development strategy and the growing demand for energy-saving and carbon-reducing innovations in the transportation sector, it is crucial to conduct in-depth research on the carbon emission factors associated with EMU operation. This will facilitate the optimization of high-speed railway EMU operation and maintenance schedules, helping high-speed railway operation management departments to develop scientifically efficient, green, and energy-saving EMU operation and maintenance schedules. Ultimately, this research aims to enhance the operational safety and energy efficiency of EMUs.

In fact, the essence of optimizing the EMU operation and maintenance schedules lies in determining the number of EMUs to be deployed and formulating maintenance schedules based on passenger travel demand and train operation schemes. The goal is to improve passenger service quality and optimize resource allocation, thereby saving resources and improving efficiency. Currently, research on EMU operation optimization mainly focuses on model construction, solution algorithm design, and collaborative optimization of operation schedules. For example, Zhong et al. [1] established a mixed-integer linear programming model for EMU operation optimization based on train schedules, with the optimization objectives of minimizing total operational costs and empty running mileage. They also designed an iterative approximation algorithm framework based on path generation to quickly obtain EMU operation schedules that satisfy daily maintenance. Gao et al. [2] addressed the coupling and uncoupling requirements in route schedules and constructed two linear integer programming

models based on paths and arcs, respectively. Lin et al. [3] built an optimization model aiming to minimize the number of EMUs required for all route schedules, with the secondary goal of minimizing total route time, and solved the model using the Gurobi solver. Zhou [4] studied the coordinated adjustment of EMU operation schedules and crew schedules under different disturbance scenarios. Tong et al. [5] proposed a continuity reliability method to optimize the task continuity reliability by analyzing the EMU operation performance in case of delays. He et al. [6] considered fluctuations in passenger flow and constraints such as EMU connection and maintenance, establishing a model and designing a Lagrangian relaxation algorithm based on the model's divide-and-conquer structure. Kang et al. [7] studied the adjustment of EMU operation schedules in response to uncertainties caused by emergencies, such as large-scale adjustments or cancellations of trains due to pandemics, proposing response and recovery strategies. Dai et al. [8] introduced carbon emission factors into the intercity railway train scheduling problem, analyzing the impact of train frequency and weighting coefficient ratios on carbon emissions and providing suggestions to control train frequency and increase the distance between large and small routes to reduce carbon emissions. Yang [9] and Luo [10] studied EMU operation under the "one-day, one-timetable" mode. Yang focused on adjusting the peak of macro passenger flow during the adjustment period and constructed an optimization model for short-period operation schedules, while Luo considered EMU turnover utilization and developed an optimization model for the coordination of EMU operation diagrams and route schedules. Miandoab et al. [11] studied the intercity railway network train operation scheduling problem with the goal of reducing carbon emissions, proposing a mixed-integer nonlinear model for the simultaneous scheduling optimization of both passenger and freight trains on intercity railways.

In addition to the aforementioned studies that focus on constructing planning models, Petri net models can also be utilized for research in the field of EMU scheduling. The method mentioned by Noulamo et al. [12] provides a reference for modeling EMU operations. Furthermore, other scholars have noted the space-time dynamic characteristics of train operation schedules and introduced space-time networks for further research. Martin-Iradi et al. [13] constructed a space-time network graph and introducing path-based 0-1 variables to model periodic train operation diagrams, and designed an algorithm for path generation to solve the model. Chen et al. [14] abstracted the EMU operation schedule as a two-dimensional space-time network and established a 0-1 integer programming model to minimize the number of EMUs used based on this network, using the Cplex solver for optimization. Qin et al. [15] established an intercity high-speed railway train scheduling optimization model based on space-time networks and designed a two-layer simulated annealing algorithm for solving the model. Zhang et al. [16] extended a space-time network structure in EMU scheduling, addressing overtaking issues by setting virtual stations to divide long intervals into shorter ones, and designed a solution algorithm based on alternating direction multipliers. Li et al. [17] established an optimization model for intercity railway EMU route schedules based on time-axis networks and designed an iterative solving method embedded in the Cplex solver. Cao [18] transformed the route planning and optimization problem into one where the operating states of trains are inserted with other EMU states in a space-time state network to form several sets, and designed a phased optimization algorithm to solve it.

Additionally, in the study of EMU operations, passenger factors can also be considered. Wan et al. [19] proposed a method for passenger flow prediction, which can be utilized. Furthermore, the methods proposed by Liu et al. [20] and El-Ajou et al. [21] can be applied to research on dynamic ticket pricing.

In summary, current research on EMU operation plan optimization mostly uses integer programming models or two-dimensional space-time network models with limited information. Solutions mainly involve heuristic algorithms or commercial solvers (such as Gurobi, Cplex, etc.). Based on this, the study combines the advantages of space-time networks in visualization analysis, accurate modeling, and multi-objective optimization. It comprehensively considers carbon emission factors in the operation and maintenance of high-speed railway EMUs under network conditions, and constructs a three-dimensional space-time network optimization model for EMU operation and maintenance. The study aims to explore the impact of carbon emissions on the preparation and optimization of EMU operation schedules.

## II. Description of EMU Operation Plan Based on Three-Dimensional Space-Time Network

Space-Time networks, are complex network models that integrate both time and spatial factors. "A train schedule diagram, or timetable, visually represents train operations. In this diagram, the horizontal axis signifies time, and the vertical axis signifies stations, inherently exhibiting two-dimensional space-time characteristics." Previous research has directly translated EMU operation schedules into two-dimensional space-time networks, where nodes represent individual EMUs, and arcs represent the space-time state changes as the EMU travels from one station to another. In this approach, the arrangement of the EMU operation schedule is considered as the selection of different state arcs in the space-time network.

However, such two-dimensional space-time network models contain very limited information and fail to effectively capture important factors such as the maintenance status, the number of maintenance events, and carbon emissions associated with EMU operations. To address these limitations, a three-dimensional space-time state network is constructed by adding a maintenance status dimension to the traditional two-dimensional space-time network. The diagram illustrating this is shown in Fig 1 below.

This model offers a more comprehensive representation of the EMU operation schedule, incorporating the usual space-time changes, the dynamic maintenance statuses and carbon emission factors, which are crucial for optimizing the operation and maintenance schedules.

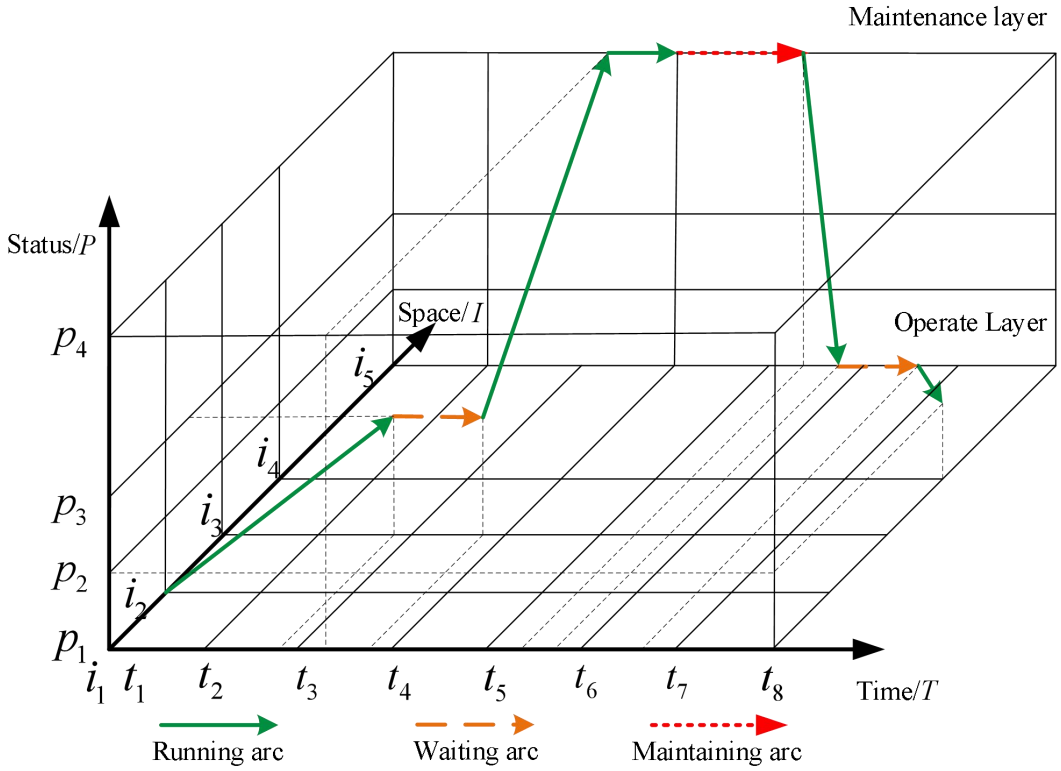


Fig.1 Three-dimensional space-time state network

In the three-dimensional network diagram shown in Fig 1, there are three axis: the time axis $T$, the space axis: $I$, and the state axis: $P$. Specifically:

The time axis $T$ represents uniformly discrete time points. This paper uses a discrete time interval of 1 minute; therefore, there are 1,440 points on the time axis T (since there are 1,440 minutes in a day).

The space axis $I$ has two meanings. In the operation layer, it represents the stations where the train is located. In the maintenance layer, it represents the EMU segment or depot adjacent to the station.

The state axis $P$ represents the maintenance status corresponding to the accumulated operation mileage and operating hours of the EMU, with values ranging from 0 to 1. When $P$ =1, it indicates that maintenance is required, corresponding to the maintenance layer, in this case, it corresponds the plane where $p_4$ is located in Fig 1. Otherwise, when $P$ is not equal to 1, it represents the operation layer, for example, the plane corresponding to the $p_2$ and $p_3$ are an operation layer.

As shown in Fig 1, the continuity and changes in the connections between running arcs, waiting arcs, and maintaining arcs clearly and comprehensively describe the space-time state changes throughout the EMU operation and maintenance process. For example, the plane corresponding to $p_4$ represents the maintenance layer, where the EMU departs from station $i_2$ and arrives at station $i_3$ (running arc).After stopping and performing operations (waiting arc), it continues to station $i_5$ (running arc) then enters the depot adjacent to the stations $i_5$ (running arc) for maintenance (maintaining arc).After maintenance is completed, the EMU returns to station $i_5$ (running arc) to continue with the next task.

In this paper, the three-dimensional space-time network model described above is used, taking into account the carbon emissions factors in the high-speed railway EMU operation process, to construct an optimization model for EMU operation schedules.

## III. MODEL BUILDING

### *A. Model Assumptions and Parameter Description*

To accurately describe the problem, the following assumptions are made for the model:

(1) The passenger demand for the high-speed railway operating section is known, and the train operation schedules for the corresponding EMUs has been determined and will not change. However, the specific EMUs and the number of them that will undertake the duties are yet to be determined.

(2) The maintenance of EMUs is permitted to be carried out at different locations. Since maintenance plans need to be developed separately for maintenance levels above Level 2, only Level 1 maintenance is considered here. In other words, no distinction is made between different maintenance levels for EMUs.

(3) The impact of EMU speed classification on train set operation is ignored, meaning the speed differences between trains are not considered;

(4) EMUs do not run on fixed sections.

The relevant variables and parameters, along with their definitions and explanations, are listed in Table I below:

TABLE I
PARAMATER INFORMATION TABLE

| Symbol | Definitions |
|---|---|
| $R=\{r_1,r_2,r_3,\cdots\}$ | Set of EMUs |
| $V=\{v_1,v_2,v_3,\cdots\}$ | Set of tasks |
| $N_s=\{n_{s1},n_{s2},n_{s3},\cdots\}$ | Set of nodes in the operation layer of the space-time networks |
| $N_d=\{n_{d1},n_{d2},n_{d3},\cdots\}$ | Set of nodes in the maintenance layer of the space-time networks |
| $N=\{n_1,n_2,n_3,\cdots\}$ | Set of all nodes in the space-time network, $N=N_s\cup N_d$ |
| $n_d^{pre}$ | Current number of EMUs that maintenance depot $n_d$ can accommodate for repair |
| $n_d^{cap}$ | Maximum number of EMUs that maintenance depot $n_d$ can accommodate for repair |
| $Z_{i,j,t,s,p,q}=\{z_1,z_2,z_3,\cdots\}$ | Set of all conflicting arcs of arc $(i,j,t,s,p,q)$ in the space-time state network |
| $U_{run}$ , $U_{wait}$ , $U_{main}$ | Set of run arcs, waiting arcs, and maintenance arcs in space-time networks |
| $U$ | Set of all arcs in the space-time state network, $U=U_{run}\cup U_{wait}\cup U_{main}$ |
| $U_{rv}$ | Set of arcs representing operational tasks in the space-time network, $U_{rv}\subset U_{run}$ |
| $(i,t,p)$ , $(j,s,q)$ | Nodes in space-time networks |
| $(i,j,t,s,p,q)$ | Arc segment from node $(i,t,p)$ to node $(j,s,q)$ in space-time network |
| $x_{i,j,t,s,p,q}^r$ | 0-1 variable, where the value is 1 if EMU r performs the operational task corresponding to arc segment $(i,j,t,s,p,q)$, otherwise, the value is 0 |
| $y_{i,j,t,s,p,q}^r$ | 0-1 variable, where the value is 1 if EMU r performs the operational task corresponding to arc segment $(i,j,t,s,p,q)$ that requires maintenance; Otherwise, the value is 0 |
| $T_{i,j,t,s,p,q}^r$ | The time required (in minutes) for EMU r to perform the operational tasks corresponding to arc segment $(i,j,t,s,p,q)$ |
| $L_{i,j,t,s,p,q}^r$ | The distance (in kilometers) traveled by the EMU r while performing the operational task corresponding to arc segment $(i,j,t,s,p,q)$ |
| $T_{common}$ | The minimum transfer time (in minutes) required for the normal connection of EMUs |
| $T_{maintain}$ | The minimum transfer time (in minutes) required for the maintenance connection of EMUs |
| $T_d^i$ | The minimum departure interval time (in minutes) at station $i$ |
| $T_a^j$ | The minimum arrival interval time (in minutes) at station $j$ |
| $T_m$ | The time required (in minutes) to perform a maintenance |
| $ML$ | The maximum operational distance (in kilometers) allowed for EMU before the next maintenance |
| $MT$ | The maximum operational time (in minutes) allowed for EMU before the next maintenance |
| $P$ | The power consumption (in kW) during the operation of the EMU |
| $P_1$ | The traction power (in kW) during the operation of the EMU |
| $P_2$ | The lighting power consumption (in W) during the operation of the EMU |
| $P_3$ | The air conditioning power consumption (in W) during operation of the EMU |
| $P_4$ | The power consumption of the signaling system during operation of the EMU |
| $\mu$ | The proportion of thermal power generation, 0.8 |

*B. Constraints for the optimization problem*

*Maintenance status constraints*

When the EMU completes a previous operational task, before taking on the next task, its accumulated mileage and operation time must be checked to see if they exceed the maintenance mileage and operation time standards, in order to determine whether maintenance is needed. The total operating mileage constraint of the EMU is given by equation (1), and the operation time constraint is given by equation (2).

$$\begin{cases} \sum_{r\in R}\sum_{(i,j,t,s,p,q)\in U_{run}} \\ L^r_{i,j,t,s,p,q}\cdot x^r_{i,j,t,s,p,q}\cdot\left(1-y^r_{i,j,t,s,p,q}\right)\le ML \\ if\ y^r_{i,j,t,s,p,q}=0 \\ x^r_{i,j,t,s,p,q}=0 \qquad if\ y^r_{i,j,t,s,p,q}=1 \end{cases} \tag{1}$$

$$\begin{cases} \sum_{r\in R}\sum_{(i,j,t,s,p,q)\in U_{run}} \\ T^r_{i,j,t,s,p,q}\cdot x^r_{i,j,t,s,p,q}\cdot\left(1-y^r_{i,j,t,s,p,q}\right)\le MT \\ if\ y^r_{i,j,t,s,p,q}=0 \\ x^r_{i,j,t,s,p,q}=0 \qquad if\ y^r_{i,j,t,s,p,q}=1 \end{cases} \tag{2}$$

*Unique occupancy constraint*

In the space-time network, at any given time, each EMU can occupy at most one arc. Similarly, each arc can be occupied by at most one EMU at any given time.

$$\sum_{r\in R} x^r_{i,j,t,s,p,q}\le 1 \quad \forall\left(i,j,t,s,p,q\right)\in U \tag{3}$$

$$\sum_{(i,j,t,s,p,q)\in U} x^r_{i,j,t,s,p,q}\le 1 \quad \forall r\in R \tag{4}$$

*The operation task can only be executed once.*

To meet transportation demand, each operation task must be executed by only one EMU once.

$$\sum_{r\in R}\sum_{(i,j,t,s,p,q)} x^r_{i,j,t,s,p,q}=1 \quad \forall v\in V \tag{5}$$

*Continuation time constraint*

Before an EMU executes the next operation task, it must check whether the connection requirements are met. If no maintenance is required, the ordinary connection constraint should be satisfied, as shown in equation (6). Otherwise, the maintenance connection constraint must be satisfied, as shown in equation (7).

$$\begin{aligned} &\left(s-t\right)\cdot x^r_{i,j,t,s,p,q}\ge T_{common} \\ &\forall r\in R \quad \forall\left(i,j,t,s,p,q\right)\in U_{wait} \end{aligned} \tag{6}$$

$$\begin{aligned} &\left(s-t\right)\cdot x^r_{i,j,t,s,p,q}\ge T_{maintain} \\ &\forall r\in R \quad \forall\left(i,j,t,s,p,q\right)\in U_{main} \end{aligned} \tag{7}$$

*Maintenance capacity constraint*

At any given time, the number of EMUs entering the maintenance depot for repair must not exceed its capacity limit.

$$\begin{aligned} &\sum_{r\in R}\sum_{(i,j,t,s,p,q)\in U_{run}} x^r_{i,j,t,s,p,q}- \\ &\sum_{r\in R}\sum_{\left(i^*,j^*,t,s,p,q\right)\in U_{run}} x^r_{i^*,j^*,t,s,p,q}+n^{pre}_d\le n^{cap}_d \\ &\forall i,j^*\in n_s \quad \forall i^*,j\in n_d \end{aligned} \tag{8}$$

In the formula: $i^*$ , $j^*$ is different from $i$ , $j$ .

*Train arrival and departure interval constraint*

In a certain section, the departure time and arrival time of the EMU's operating tasks must meet the minimum departure interval and minimum arrival interval requirements to avoid collisions or other accidents.

$$\begin{cases} \sum_{r\in R}\sum_{z\in Z_{i,j,t,s,p,q}} x^r_{i,j,t,s,p,q}=1 \\ Z_{i,j,t,s,p,q}= \\ \left\{\left(i,j,t,s,p,q\right)\middle|\left|t-t^*\right|<T^i_d,\left|s-s^*\right|<T^j_a\right\} \\ \forall\left(i,j,t,s,p,q\right)\in U_{run} \end{cases} \tag{9}$$

In the formula, $t^*$ and $s^*$ are the start and end times of the operating tasks corresponding to the arc $\left(i,j,t,s,p,q\right)$ when a conflict occurs.

*Decision variable value constraint*

$$\begin{aligned} &x^r_{i,j,t,s,p,q}\in\{0,1\} \\ &\forall r\in R \quad \forall\left(i,j,t,s,p,q\right)\in U \end{aligned} \tag{10}$$

$$\begin{aligned} &y^r_{i,j,t,s,p,q}\in\{0,1\} \\ &\forall r\in R \quad \forall\left(i,j,t,s,p,q\right)\in U \end{aligned} \tag{11}$$

## C. Objective Function

The objective function consists of three parts

*Goal I: Minimize the total operation time of all EMUs*

$$\min Z_1=\sum_{r\in R}\sum_{(i,j,t,s,p,q)\in U} T^r_{i,j,t,s,p,q}\cdot x^r_{i,j,t,s,p,q} \tag{12}$$

Under the premise of satisfying all constraints, minimize the total operation time of all EMUs, including their running, waiting, and maintenance times.

*Goal II: Minimize the number of maintenance occurrences*

$$\min Z_2=\sum_{r\in R}\sum_{(i,j,t,s,p,q)\in U} y^r_{i,j,t,s,p,q} \tag{13}$$

A reasonable maintenance frequency can improve the operational efficiency of EMUs and ensure the safe execution of operational tasks, but excessive maintenance frequency will, to some extent, increase the number of EMUs used.

*Goal III: Optimal carbon emissions balance*

The carbon emissions calculation, based on the method proposed by Long [22] for railway transit, is as follows:

According to the national energy statistics report, for every 1 kW·h of electricity, approximately 345g of standard coal is required. The combustion value of standard coal is 29.3 MJ/kg, and the emission coefficient of raw coal is 94,600 kg/TJ (measured in $CO_2$). Therefore, the carbon emissions calculation formula can be derived as follows:

$$\begin{aligned} &\text{Carbon emissions} = \\ &\mathrm{E}\times\mu\times 0.345\mathrm{kg}\times 29.3\,MJ/\,kg\times 94600\,kg/\,TJ \end{aligned} \tag{14}$$

In the formula, $E$ represents the electricity consumption during railway transit operation, and $\mu$ represents the proportion of electricity generated by thermal power. The electricity consumption primarily stems from the train traction and station equipment, while the power usage of station air conditioning, lighting, and other equipment remains relatively fixed and does not change with the operating schedule [8]. Therefore, the electricity consumption of the train's air conditioning, lighting, signaling system, and traction are all included in the total electricity consumption during the train's operation.

According to reference [22], the electricity consumption of the train's air conditioning, lighting, and signaling systems is shown in equation (15), (16), (17).

$$P_2 = n_1 \times \mathrm{n}_2 \times 40 \tag{15}$$

$$P_3 = s \times 2 \times T \times 3 \times n_2 \tag{16}$$

$$P_4 = n_2 \times 2 \times 230 \tag{17}$$

In the formula, $n_1$ : Number of lighting fixtures in a single carriage; $n_2$ : Number of carriages; $s$ : Surface area of a single carriage; $T$ : Temperature difference between inside and outside.

Overall, the electricity consumption during the train's operation period is shown in equation (18).

$$P = P_1 + \left(P_2 + P_3 + P_4\right) \times 10^{-3} \tag{18}$$

The total carbon emissions for a train during its entire operational period can be calculated as in equation (19).

$$carbon = \sum_{r \in R} \sum_{(i,j,t,s,p,q) \in U} T^r_{i,j,t,s,p,q} \cdot x^r_{i,j,t,s,p,q} \cdot P \cdot \mu \times 0.345 \times 29.3 \times 94600 \times 10^{-6} \tag{19}$$

Therefore, the sum of the absolute differences between the carbon emission of each EMU and the average carbon emission of all EMUs serves as the balance measure. The smaller this value, the more balanced the carbon emissions are there.

$$\min Z_3 = \sum_{r \in R} \left| \frac{\sum_{(i,j,t,s,p,q) \in U} carbon \cdot x^r_{i,j,t,s,p,q} - \sum_{r \in R} \sum_{(i,j,t,s,p,q) \in U} carbon \cdot x^r_{i,j,t,s,p,q}}{N(R)} \right| \tag{20}$$

In the formula: $N(R)$ represents the total number of EMUs

## IV. Algorithm Design and Model Solving

Given that the model is a non-convex multi-objective mixed-integer programming model, it is difficult to solve using exact algorithms. Therefore, a heuristic algorithm is designed for solving the problem. For the maintenance process mentioned in the paper, the segmentation approach proposed by Loresco et al. [23] can be used for further research. The NSGA-II algorithm, proposed by Deb et al. [24], is an improved version of the NSGA algorithm, which uses a fast non-dominated sorting method. This not only reduces the algorithm's complexity but also effectively decreases the computation time. The algorithm introduces an elitism strategy by combining parent and offspring populations, allowing individuals to be selected from a larger search space. This ensures that high-quality individuals are not discarded during the evolutionary process, thereby improving the accuracy of optimization results and the robustness of the algorithm. Additionally, when addressing multi-objective problems, it eliminates the need for manual weight settings, avoiding the subjective bias introduced by weight allocation. This makes NSGA-II a highly efficient algorithm for solving multi-objective optimization problems.

Given the problem and model characteristics, an improved NSGA-II algorithm is designed to adapt to the three-dimensional space-time model. The flowchart of the algorithm is as shown in Fig 2:

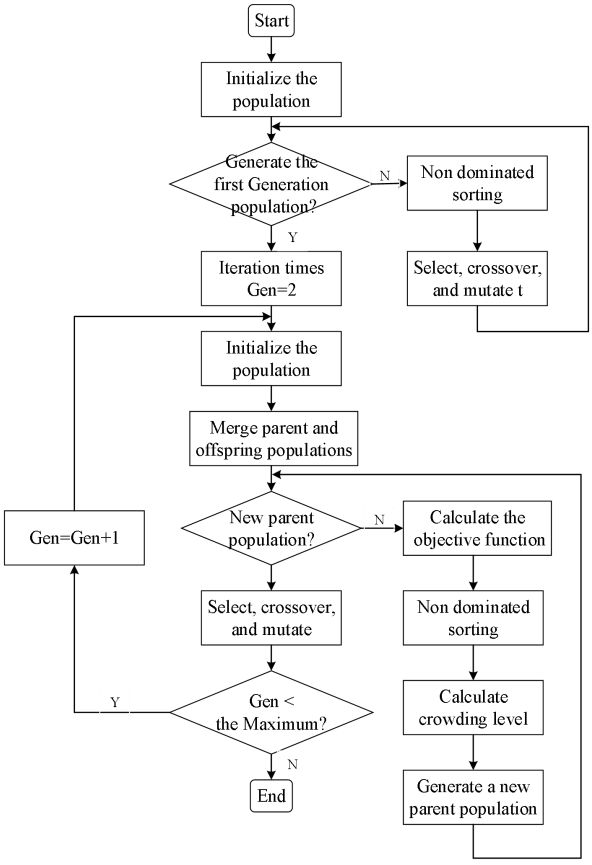


Fig.2 NSGA-II Algorithm Process

### A. Code

Based on the three-dimensional space-time states characteristics, and the properties of the 0-1 variables $x^r_{i,j,t,s,p,q}$ and $y^r_{i,j,t,s,p,q}$ , a three-dimensional array $m \times n \times k$ is designed to serve as a chromosome. This chromosome represents the selection of m EMUs for n arcs in the space-time network, with k representing the maintenance status of the EMUs. Specially, for the 0-1 variable $y^r_{i,j,t,s,p,q}$ , the value of the k is set to 2, which represents a specific state of maintenance or other relevant operation in the space-time network.

The decision variables of the model are $x^r_{i,j,t,s,p,q}$ and $y^r_{i,j,t,s,p,q}$ , which respectively represent whether an EMU perform a certain operational task (arc) and whether it executes a maintenance task for that arc. Since there are two decision variables and the maintenance state $k$ set the value to 2, the designed three-dimensional array chromosome encoding can be visualized as the vertical concatenation of two $m \times n$ matrices, where the first matrix the decision variable $x^r_{i,j,t,s,p,q}$ and the second matrix represents the decision variable $y^r_{i,j,t,s,p,q}$ . The feasible solution structure of the model is shown in equations (21) and (22):

$$X=\begin{bmatrix} x_{11} & x_{12} & \cdots & x_{1n} \\ x_{21} & x_{22} & \cdots & x_{2n} \\ \cdots & \cdots & \cdots & \cdots \\ x_{m1} & x_{m2} & \cdots & x_{mn} \end{bmatrix} \tag{21}$$

$$Y=\begin{bmatrix} y_{11} & y_{12} & \cdots & y_{1n} \\ y_{21} & y_{22} & \cdots & y_{2n} \\ \cdots & \cdots & \cdots & \cdots \\ y_{m1} & y_{m2} & \cdots & y_{mn} \end{bmatrix} \tag{22}$$

### *B. Crossover and Mutation*

Common crossover operations include cyclic crossover, order-based crossover, and others. These methods usually help maintain genetic diversity and avoid repetition. However, if this algorithm continues to use the above crossover methods, conflicts may arise between the crossover point information and the subsequent chromosome information, or the constraints may not be met. Therefore, based on the characteristics of the research problem and the 3D encoding method, corresponding improvement strategies are used to ensure the correctness and uniqueness of the genes.

(1) The crossover operation is performed on the plane representing the 0-1 variable $x^{r}_{i,j,t,s,p,q}$ using the tournament selection method, which means the crossover operation is applied to the $X$ matrix without involving maintenance. Two parent individuals are selected for crossover, and an EMU is randomly chosen as the crossover point in each parent's chromosome. The genetic information at the crossover points is then exchanged between the two parents.

(2) After the crossover operation, the offspring are checked and modified to ensure they meet the constraint conditions. Since each operation task can only be executed once, after crossover, priority is given to ensuring that the genes resulting from the crossover remain unchanged. Subsequently, other genes are checked. When the information of a gene satisfies the constraints, it is not altered; if there is an overlap in the gene information, meaning the operation task for that arc has already been assigned to another EMU, the gene information before that point is retained, while the information at and after that point is deleted. After all genes are checked, if any operation task has not been executed, the corresponding information for the unexecuted tasks is added to the chromosome, ensuring that it satisfies the constraint conditions. This approach ensures that the chromosome information carried by the offspring generated through crossover always satisfies the constraints.

To clarify, let's consider a scenario with 2 stations, 6 EMUs, and 14 operation tasks, with the time period from 6:00 to 24:00 (18 hours), and a discrete time interval of 1 hour. A corresponding three-dimensional space-time network is constructed, and the crossover process is explained using the network diagrams shown in Fig 3, 4, and 5.

In this case, the space-time network contains 2 nodes and 19 time points. The total number of possible arc segments in the network is calculated as 2 × (2-1) × 19 = 38, which forms a 6 × 38 matrix. To simplify, since the crossover operation does not involve maintenance and only concerns the operation arcs corresponding to tasks, this can be reduced to a 6 × 14 matrix.

The offspring generated from the crossover operation are shown in Fig 4 .In Offspring 1, arc segments 2 and 9 are duplicated, and arc segments 4 and 11 were executed. In Offspring 2, arc segments 4 and 11 are duplicated, while arc segments 2 and 9 were not executed, both of which violate the demand constraints.

Thus, Offspring 1 and Offspring 2 are modified to satisfy the constraints, and new offspring are generated, as shown in Fig 5.

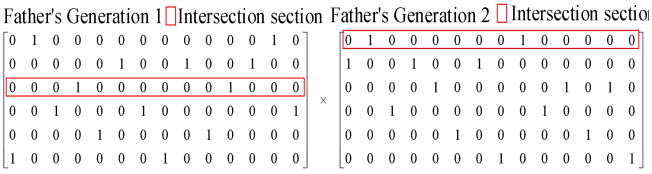


Fig.3 Cross parent

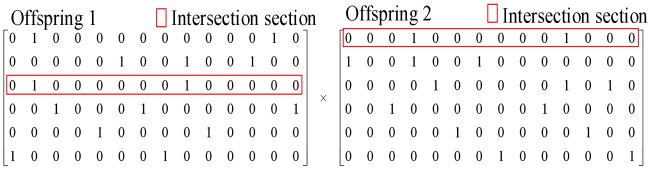


Fig.4 Cross offspring

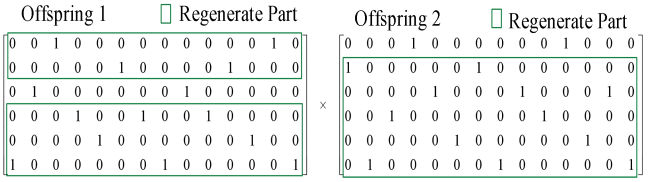


Fig.5 Regenerate non intersecting parts

(3) The algorithm adopts a uniform mutation strategy, where each gene in the chromosome is replaced by new information based on a certain probability. Unlike crossover operations, the mutation operation occurs on both the planes representing the 0-1 variables $x^{r}_{i,j,t,s,p,q}$ and $y^{r}_{i,j,t,s,p,q}$, meaning both the execution of operation tasks and maintenance of EMUs may undergo mutation. After the mutation, similar to the crossover, the offspring chromosome must be checked to ensure it meets the constraint conditions.

Other steps of the algorithm, such as tournament selection, non-dominated sorting, crowding distance calculation, and elite retention strategies, are the same as the original NSGA-II algorithm and will not be repeated here.

## V. Example Calculation

To verify the effectiveness of the model and algorithm, data from the operation plan of the Beijing-Shanghai High-Speed Railway for the first quarter of 2021, including both line and some interline EMU train services, were selected. The data comprised 120 train tasks, with 59 down-bound and 61 up-bound trains, utilizing a total of 55 EMUs to complete the involved train tasks. The operation plan was referenced from the existing EMU schedule plan for the Beijing-Shanghai High-Speed Railway line [25]. The

operation plan (with station stopping scheme omitted)is shown in Fig 6.

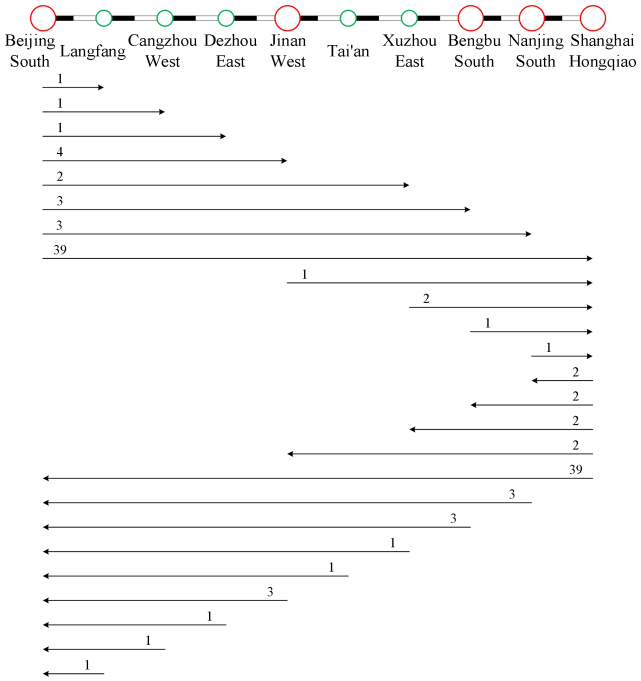


Fig.6 Train operation schedules for the Beijing Shanghai High-Speed Railway (station stopping scheme omitted)

In this paper, a unified 16-carriage train composition is used, the EMUs have a uniform speed grade and are operated on fixed sections. Additionally, the minimum departure interval and the arrival tracking interval are both set to 4 minutes, i.e., $T_d^i = T_a^j = 4$ min. The parameter values required for solving the example using the NSGA-II algorithm are shown in Table II.

TABLE II
PARAMATER INFORMATION TABLE

| Parameter | Value |
|---|---|
| $T_{common}$ | 15min |
| $T_{maintain}$ | 180min |
| $T_m$ | 150min |
| $ML$ | 48h |
| $MT$ | 5500km |
| Population size $npop$ | 50 |
| Cross probability $pc$ | 0.8 |
| Mutation probability $pm$ | 0.04 |
| Maximum number of iterations $\max it$ | 100 |

The NSGA-II algorithm was executed using MATLAB R2020b on a personal computer with a Windows 11 (64-bit) operating system, Intel(R) Core(TM) i7-9750H CPU @ 2.60GHz, and 16GB of RAM. The computation time was 694.5 seconds. The calculation results are shown in Table III, which presents the Pareto solution set data after eliminating invalid solutions.

TABLE III
PARETO DATASET

| Solution | Total Operating Time of EMUs | Maintenance Frequency | Carbon Emission Quota |
|---|---|---|---|
| 1 | 547816 | 15 | 1292802.67 |
| 2 | 567552 | 11 | 1234908.01 |
| 3 | 588247 | 16 | 1010299.07 |
| 4 | 547891 | 14 | 1469223.36 |
| 5 | 568411 | 18 | 1093097.82 |
| 6 | 588348 | 15 | 1074328.85 |
| 7 | 587737 | 12 | 1180707.74 |
| **8** | **557593** | **11** | **1293171.28** |
| 9 | 578317 | 16 | 1068555.77 |
| 10 | 547998 | 15 | 1215705.90 |
| 11 | 578702 | 18 | 1060317.22 |
| 12 | 557850 | 13 | 1234263.29 |
| 13 | 577668 | 13 | 1184128.55 |
| 14 | 577737 | 12 | 1189560.28 |
| 15 | 567846 | 13 | 1226401.83 |
| 16 | 577868 | 14 | 1133198.49 |
| 17 | 588236 | 16 | 1060056.14 |
| 18 | 557793 | 14 | 1271357.26 |
| 19 | 568066 | 15 | 1101554.93 |
| 20 | 567954 | 15 | 1173673.85 |
| 21 | 577721 | 14 | 1143958.59 |
| 22 | 567849 | 13 | 1200887.33 |
| 23 | 557646 | 14 | 1272749.29 |
| 24 | 557763 | 12 | 1289603.08 |
| 25 | 587775 | 13 | 1082211.50 |
| 26 | 568289 | 15 | 1097846.47 |
| 27 | 577851 | 14 | 1137763.92 |
| 28 | 578411 | 15 | 1078096.46 |
| 29 | 567710 | 14 | 1227836.84 |
| 30 | 567847 | 12 | 1218274.36 |
| 31 | 578050 | 15 | 1087238.31 |
| 32 | 568060 | 14 | 1195804.46 |

Notes: the units for the total operating time and maintenance frequency of EMU are min and kg, respectively

From Table III, it can be observed that the optimal solutions for the three objectives do not appear simultaneously in a single solution. Moreover, there is no solution in the Pareto set that dominates all other solutions across the three optimization objectives. In other words, all solutions in the Pareto set are non-dominated.

TABLE IV
OPTIMIZED BEIJING-SHANGHAI HIGH SPEED RAIWAY ROUTE

| EMU number | route | maintenance after completed the task | EMU number | route | maintenance after completed the task |
|---|---|---|---|---|---|
| 6001 | G7802-G143-G4 | G4 | 6027 | G104-G133 | |
| 6002 | G7804-G111-G144-G337 | | 6028 | G336-G7-G152 | |
| 6003 | G8936-G113-G14 | G14 | 6029 | G116-G147 | |
| 6004 | G338-G121-G154 | | 6030 | G6-G137 | G137 |
| 6005 | G208-G123-G156 | G156 | 6031 | G262-G9-G7190 | |
| 6006 | G7709-G22 | | 6032 | G114-G155 | |
| 6007 | G126-G273 | G273 | 6033 | G131-G7176 | |
| 6008 | G112-G141 | G141 | 6034 | G7764-G7279 | |
| 6009 | G135 | | 6035 | G5-G12-G17 | |
| 6010 | G10-G169 | | 6036 | G140-G8935 | |
| 6011 | G352-G161 | G161 | 6037 | G102-G23-G30 | |
| 6012 | G107-G142-G7801 | | 6038 | G106-G139 | G139 |
| 6013 | G120-G43-G7765 | | 6039 | G115-G168 | |
| 6014 | G117-G148 | | 6040 | G110-G145 | |
| 6015 | G103-G136-G269 | | 6041 | G334-G411-G160 | |
| 6016 | G170 | | 6042 | G162-G157 | |
| 6017 | G105-G138-G207 | G207 | 6043 | G7180-G274-G159 | |
| 6018 | G7178-G2-G351 | G351 | 6044 | G108-G3 | G3 |
| 6019 | G127-G7710 | | 6045 | G118-G151 | |
| 6020 | G412-G203 | | 6046 | G109-G7280 | |
| 6021 | G125-G158 | | 6047 | G2661-G124-G267 | |
| 6022 | G1210 | | 6048 | G8-G11 | |
| 6023 | G1-G146-G7803 | | 6049 | G101-G134-G341 | |
| 6024 | G132-G331 | | 6050 | G2662 | |
| 6025 | G122-G13 | | 6051 | G24-G149 | |
| 6026 | G119-G16 | | 6052 | G128-G153 | |

In Table III, solution 1 has the least total operating time for the EMUs, at 547,865 seconds; solutions 2 and 8 have the fewest maintenance instances, with 11 instances; and solution 3 has the best carbon emission balance, with a value of 1,010,299.07 kg. Although each solution in the Pareto set excels in one of the optimization goals, they are all optimal under the NSGA-II improved algorithm framework, with different preferences for each objective. Therefore, the decision-maker can select an appropriate solution from the Pareto set based on real-world needs or preferences.

Taking into account the total operation time of EMUs, the total number of maintenance times, and the balanced carbon emission indicators corresponding to each solution in Table 3, Solution 8 is selected as the optimal solution for this case. This solution has a total EMUs operation time of 557,593 seconds, the total number of maintenance times is 11 times, and the balanced carbon emission indicators value of 1,293,171.28 kg. Among all the solutions, Solution 8 has the fewest total maintenance times for EMUs. Although its total operation time and balanced carbon emission indicators are not the best among all alternative solutions, they still represent relatively good choices compared to the other options.

The calculation results show that only 52 EMUs are needed to meet all the transportation demands of the Beijing-Shanghai High-Speed Railway in one day. These transportation demands include only the operation tasks where both the departure and arrival stations are among the 24 stations along the Beijing-Shanghai High-Speed Railway. Operation tasks not meeting this condition are not considered for the time being.

Compared with the original data, the calculation results in this paper save 3 EMUs. The optimized EMU routing scheme for the Beijing-Shanghai High-Speed Railway is shown in Table IV, and the corresponding EMUs routing diagram is shown in Fig 7. The 10 stations shown in Fig 7 are all stations with departure or arrival tasks, and the other 14 stations are omitted.

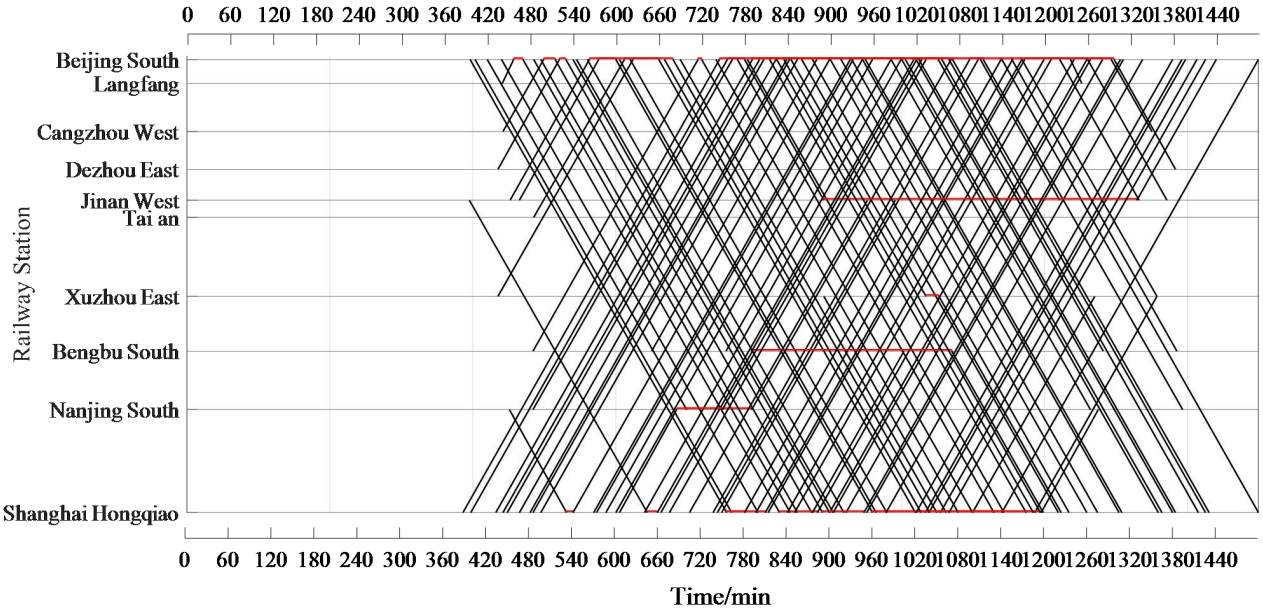


Fig.7 Optimized Beijing-Shanghai High-Speed Railway EMUs routing diagram

Based on the Pareto solutions obtained from the NSGA-II algorithm, the corresponding Pareto frontier graph is shown in Fig 8.

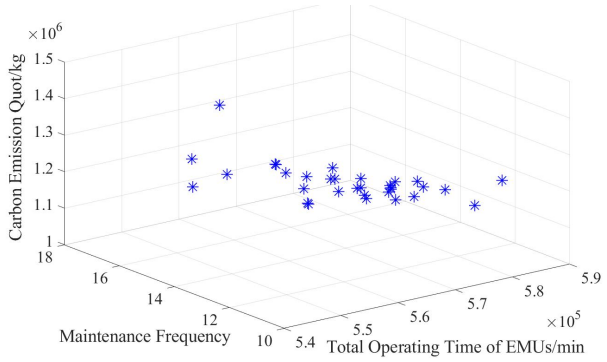


Fig.8 Pareto Frontier

From Fig 8, it is evident that the optimal solution initially shows a decrease in carbon emissions as the total EMU operating time increases and the maintenance frequency decreases. However, once the optimal state is reached, further increases in operating time lead to a gradual rise in carbon emissions. This trend aligns with the actual situation in the operation of EMUs.

This observation clearly demonstrates that the model accurately reveals the interaction mechanisms between carbon emissions, total operating time, and maintenance frequency in the process of high-speed EMU operations. It reflects how these factors influence each other, showing that while optimizing operating time and reducing maintenance frequency can lower emissions up to a point, beyond that point, further increases in operating time may lead to higher emissions, thereby illustrating a trade-off between efficiency and environmental impact.

To demonstrate the effectiveness of the model, a comparative analysis is performed from three aspects: the number of EMUs in operation, the operating time of EMUs, and the operating mileage of EMUs.

(1) Number of EMUs in operation

The existing Beijing-Shanghai High-Speed Railway has planned 55 EMU train routes. In this study, it was determined that 52 sets of EMUs serve all the trains on the Beijing-Shanghai section and some cross-line trains, saving 3 sets of EMUs. However, since only part of the cross-line trains running on the Beijing-Shanghai section were selected for this case study, the comparison between the existing EMU train schedule and the calculated schedule cannot be made solely based on the number of EMUs used. It is necessary to consider the EMU operation time utilization and travel distance for a comprehensive assessment.

(2) EMU operation time utilization rate

This paper uses the utilization rate of EMU operation time as a measure of operational efficiency. It represents the ratio of the total operation time of the EMU across various operational segments to the total operating time for a full day. This reflects the proportion of the EMU's effective operation during non-window periods. The calculation formula is as follows:

$$utilization\ rate = \frac{effective\ operation\ duration}{1440 - maitenance\ \ window} \quad (23)$$

The operational time utilization rate for each EMU route of the Beijing-Shanghai High-Speed Railway is calculated using Formula (23). The effective operation duration in this formula refers to the pure running time of a particular EMU within one day, excluding the time spent at stations and the time occupied for maintenance. The number 1440 indicates that there are 1440 minutes in a day. In this paper, the period from 0:00 to 6:00 (in 24-hour format) is designated as the maintenance window time, which amounts to 6 hours.

The results are shown in Table V.

TABLE V
THE OPERATIONAL DURATION AND UTILIZATION RATE OF EMUs ON THE BEIJING-SHANGHAI-HIGH-SPEED RAILWAY

| EMU number | Effective operation duration | Utilization rate | EMU number | Effective operation duration | Utilization rate |
|---|---|---|---|---|---|
| 6001 | 734 | 0.67963 | 6027 | 718 | 0.664815 |
| 6002 | 886 | 0.82037 | 6028 | 829 | 0.767593 |
| 6003 | 804 | 0.744444 | 6029 | 718 | 0.664815 |
| 6004 | 845 | 0.782407 | 6030 | 638 | 0.590741 |
| 6005 | 907 | 0.839815 | 6031 | 761 | 0.70463 |
| 6006 | 530 | 0.490741 | 6032 | 718 | 0.664815 |
| 6007 | 638 | 0.590741 | 6033 | 439 | 0.406481 |
| 6008 | 718 | 0.664815 | 6034 | 256 | 0.237037 |
| 6009 | 359 | 0.332407 | 6035 | 917 | 0.849074 |
| 6010 | 718 | 0.664815 | 6036 | 445 | 0.412037 |
| 6011 | 590 | 0.546296 | 6037 | 581 | 0.537963 |
| 6012 | 734 | 0.67963 | 6038 | 718 | 0.664815 |
| 6013 | 719 | 0.665741 | 6039 | 718 | 0.664815 |
| 6014 | 718 | 0.664815 | 6040 | 718 | 0.664815 |
| 6015 | 949 | 0.878704 | 6041 | 829 | 0.767593 |
| 6016 | 359 | 0.332407 | 6042 | 590 | 0.546296 |
| 6017 | 907 | 0.839815 | 6043 | 718 | 0.664815 |
| 6018 | 670 | 0.62037 | 6044 | 718 | 0.664815 |
| 6019 | 530 | 0.490741 | 6045 | 718 | 0.664815 |
| 6020 | 638 | 0.590741 | 6046 | 487 | 0.450926 |
| 6021 | 718 | 0.664815 | 6047 | 839 | 0.776852 |
| 6022 | 249 | 0.230556 | 6048 | 718 | 0.664815 |
| 6023 | 775 | 0.717593 | 6049 | 829 | 0.767593 |
| 6024 | 470 | 0.435185 | 6050 | 249 | 0.230556 |
| 6025 | 718 | 0.664815 | 6051 | 590 | 0.546296 |
| 6026 | 718 | 0.664815 | 6052 | 718 | 0.664815 |

From Table V, it can be observed that 34 sets of EMUs have a utilization rate greater than 60%, maintaining a relatively balanced state. However, 11 sets of EMUs have a utilization rate below 50%, indicating that there is still some disparity in utilization. Since the Beijing-Shanghai High-Speed Railway mainly operates long-distance trains with long travel times, each set of routes includes fewer trains, and there is limited room for adjusting train connections. Therefore, the optimization results in this study still have some room for improvement.

(3) EMU operating mileage

The EMU first-level maintenance standard used in this study is an operating mileage of 5500 km or an operating time of 48 hours. Due to the limited flexibility in adjusting train schedules and train connections on the Beijing-Shanghai High-Speed Railway, the optimization potential is constrained. However, within a maintenance cycle, different EMUs can be assigned to daily routes with varying mileages, so that the operating mileage of different EMUs in the first-level maintenance cycle can be balanced, further optimizing the balance of EMU mileage utilization.

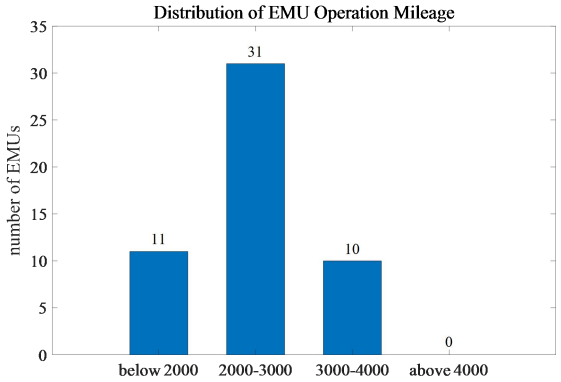


Fig 9 EMU operating mileage

Fig 9 shows the distribution of EMU route mileage across different ranges on the Beijing-Shanghai High-Speed Railway. From Fig 9, it can be observed that most EMUs are

distributed above 2000 km, with a concentration in the 2000 km to 3000 km range. This confirms that the EMU route plan ensures the balance of operating mileage for the majority of EMUs.

## VI. Conclusion

(1) Considering carbon emissions in the optimization of high-speed EMU operations is both necessary and feasible. As China actively promotes the gradual implementation of the carbon peaking and carbon neutrality goals, addressing the carbon emissions in the operation and maintenance processes of the heavily used EMUs is crucial. This approach helps to accurately assess and optimize energy efficiency during the EMU operation process, contributing to energy conservation and carbon reduction efforts in the transportation sector.

(2) Constructing an optimization model and algorithm for high-speed EMU operation schedules based on a three-dimensional space-time network is effective. Addressing the space-time state changes in the EMU operation and maintenance processes, and leveraging the advantages of the three-dimensional space-time network, a multi-objective mixed-integer programming model for EMU operation schedule optimization has been established. Based on the model's characteristics, an NSGA-II improved solution algorithm with three-dimensional information encoding was designed. This model accurately reveals the interaction mechanisms among factors such as carbon emissions, total operating time, and maintenance frequency in the operation of EMUs. This ensures that when developing EMU operation and maintenance schedules, it is possible to effectively ensure the safety performance of the EMUs, improve their operational efficiency, and also consider the carbon emission balance indicator. The improved crossover strategy ensures that constraints are met while maintaining population diversity and stability.

(3) The case study of the Beijing-Shanghai High-Speed Railway shows that the constructed model and designed algorithm are effective. The optimal solution requires only 52 EMUs to meet the operational demand, which is 3 less than the original plan of 55 EMUs, thus effectively improving the utilization rate of EMUs. In addition, a comparative analysis was conducted on the EMUs used from three aspects: the number of EMUs used, the running time of EMUs, and the mileage of EMUs. The results show that more than 60% of the EMUs have a utilization rate of over 60%, and the mileage range of EMUs is within a certain interval, indicating a high level of balance in the use of EMUs.

## References


[1] ZHONG Qingwei, ZHANG Yongxiang, WANG Dian, et al. Optimization model and algorithm for train-set scheduling based ontrip sequence[J]. Journal of Southwest Jiaotong University, 2021,56(2): 385-394

[2] GAO Y, Schmidt M, YANG L, et al. A branch-and-price approach for trip sequence planning of high-speed train units[J]. Omega, 2020, 92: 102150.

[3] LIN Boliang, SHEN Yaoming, ZHONG Wenjian, et al. Optimization of the Electric Multiple Units Circulation Plan with the Minimum Number of Train-Set [J] .China Railway Science,2023,44(5):210-221

[4] ZHOU Lingshuang, PENG Qiyuan, ZHANG Zhibo,et al. Research on Collaborative Rescheduling for Rolling Stock and Crew on High Speed Railways[J]. RAILWAY TRANSPORT AND ECONOMY, 2021,43(05):1-7.

[5] TONG Shuo, CHEN Shaokuan, LIU Gehui,et al. Optimum Circulation Model for Electrical Multiple UnitsConsidering Reliability of Their Operational Connections[J]. JOURNAL OF THE CHINA RAILWAY SOCIETY, 2020,42(04):27-34.

[6] HE Xiaoyong, WANG Ying, LI Han,et al. Study on rolling stock rescheduling under passenger demand fluctuation[J/OL]. Journal of Railway Science and Engineering,1-11[2024-07-10].

[7] KANG L, XIAO Y, SUN H, et al. Decisions on train rescheduling and locomotive assignment during the COVID-19 outbreak: A case of the Beijing-Tianjin intercity railway[J]. Decision Support Systems, 2022, 161: 113600.

[8] DAI Yanze, ZHAN Shuguang. Analysis of full-length and short-turn routing of urban railway transit considering carbon emission[J] Journal of Railway Science and Engineering,2022,19(12):3546-3556.

[9] LIN Yang. Study on Optimization of High-speed Railway Operation Planning under the Mode of "Day-New-Diagram"[D]. Beijing Jiaotong University,2022.

[10] LUO Qiang. Collaborative Optimization of Train Timetable and EMU Circulation Based on Day-New-Diagram[D]. Beijing Jiaotong University,2021.

[11] Miandoab M H, Ghezavati V, Mohammaditabar D. Developing a simultaneous scheduling of passenger and freight trains for an inter-city railway considering optimization of carbon emissions and waiting times[J]. Journal of Cleaner Production, 2020, 248: 119303.

[12] Thierry Noulamo, Emmanuel Tanyi, Marcellin Nkenlifack, Jean-Pierre Lienou, and Alain Djimeli, "Formalization Method of the UML Statechart by Transformation Toward Petri Nets," IAENG International Journal of Computer Science, vol. 45, no.4, pp505-513, 2018

[13] Martin-Ieadi B, Ropker S. A column-generation-based matheuristic for periodic train timetabling with integrated passenger routing[J]. arxiv preprint arxiv:1912.06941, 2019.

[14] CHEN Minyu, ZHANG Yujie, ZHANG Shoushuai,et al. Operation Plan Optimization of Electric Multiple Units Based on the Minimum Number of Rolling Stock[J]. RAILWAY TRANSPORT AND ECONOMY, 2022,44(08):52-57.

[15] QIN Jin, TAN Yunchao, ZHANG Wei, et al. Train Planning Optimization for Intercity Railway Based on Space-time Network[J]. JOURNAL OF THE CHINA RAILWAY SOCIETY, 2020,42(02):1-10.

[16] ZHANG Y, PENG Q, YAO Y, et al. Solving cyclic train timetabling problem through model reformulation: Extended time-space network construct and Alternating Direction Method of Multipliers methods[J]. Transportation Research Part B: Methodological, 2019, 128: 344-379.

[17] LI Jian, WANG Ying, LI Haiying, et al. Optimization model of rolling stock circulation of intercity railway[J]. Journal of Railway Science and Engineering,2018,15(07):1664-1670.

[18] CAO Wenbin. Research on Optimization of Electric Multiple Units Circulation Plan[D]. Beijing Jiaotong University,2020.

[19] Wan Zakiyatussariroh Wan Husin, Mohammad Said Zainol, and Norazan Mohamed Ramli, "Common Factor Model with Multiple Trends for Forecasting Short Term Mortality," Engineering Letters, vol. 24, no.1, pp98-105, 2016

[20] Guo Liu, Qiang Zhao, and Guiding Gu, "A Simple Control Variate Method for Options Pricing with Stochastic Volatility Models," IAENG International Journal of Applied Mathematics, vol. 45, no.1, pp64-70, 2015

[21] Ahmad El-Ajou, Zaid Odibat, Shaher Momani, and Ahmad Alawneh "Construction of Analytical Solutions to Fractional Differential Equations Using Homotopy Analysis Method," IAENG International Journal of Applied Mathematics, vol. 40, no. 2, pp43-51, 2010

[22] J,Long. Evaluation Model and Optimization Method of Urban Passenger Transport System Based on Carbon Emission Target[D]. Huazhong University of Science and Technology,2012.

[23] Lorseco P J M, Vicerra R R P, Dadios E P. "Segmentation of lettuce plants using super pixels and thresholding methods in smart farm hydroponics setup," Lecture Notes in Engineering and Computer Science: Proceedings of The World Congress on Engineering 2019,3-5 July, 2019.London, U.K, pp59-64.

[24] Deb K, Pratap A, Agrwal S, et al. A fast and elitist multiobjective genetic algorithm: NSGA-II[J]. IEEE transactions on evolutionary computation, 2002, 6(2): 182-197.

[25] ZHOU L. Research on Coordinated Optimization of High-speed Railway Timetabling and EMU Operation Scheduling[D]. Beijing Jiaotong University,2021.